Multifunctional ZnO-Biopolymer Nanocomposite Coatings for Health-Care Polymer Foams and Fabrics

P. K. Sanoop,[1] K. V. Mahesh,[1] K. M. Nampoothiri,[2] R. V. Mangalaraja,[3] S. Ananthakumar[1]

[1]*Nanoceramics Division, National Institute for Interdisciplinary Science and Technology, Council of Scientific and Industrial Research (CSIR), Thiruvananthapuram, Kerala 695019, India*
[2]*Biotechnology Division, National Institute for Interdisciplinary Science and Technology, Council of Scientific and Industrial Research (CSIR), Thiruvananthapuram, Kerala 695019, India*
[3]*Department of Engineering Materials, University of Concepcion, Concepcion, Chile*

Received 5 August 2011; accepted 16 January 2012
DOI 10.1002/app.36831
Published online in Wiley Online Library (wileyonlinelibrary.com).

ABSTRACT: Biopolymer-mediated sonochemical synthesis has been carried out for obtaining stable, nanocrystalline ZnO-biopolymer nanocomposite colloids to be applied on polymer foam and cotton fabrics to ultimately produce multifunctional, heath-care surface modifications. *In situ* nucleation and growth of nano-ZnO was achieved by ultrasonication at $\sim 60^{\circ}C$ in aqueous biopolymer media prepared using starch, gelatin, chitosan, and agar. Phase analysis, structure–bonding characteristics, ZnO morphology, particle size distributions, rheology, and thermal decompositions were studied using XRD, FTIR, SEM/TEM, viscometer, and TG/DTA tools. Morphologically varied nanocrystalline ZnO of size ~ 40 nm were synthesized. Biopolymers media resulted in stable ZnO colloids through steric stabilization. ZnO-biopolymer nanocomposites colloid was applied on polyurethane foams and cotton fabric substrates by dip coating. These coatings were examined for the UV photoactivity and resistance to fungi growth. A comparison has been made among the biopolymers. It is shown that the surface coatings of ZnO-biopolymer nanocomposites can produce anti-fungal, UV active polymer foams and fabrics. The study has significant relevance in automobile and hospital industries because such functionally modified polymer foams and cotton fabrics can be disinfected and refreshed just by periodic application of water-free, UV cleaning. J Appl Polym Sci 000: 000–000, 2012

Key words: biopolymers; coatings; nanocomposites; polyurethanes; surface modification

INTRODUCTION

Applications of nano-engineered inorganic-polymer hybrid soft-coatings on the surfaces of textiles, leather, and home appliances received wide popularity because they offer attractive multifunctional properties like oil-repellent, stain-free, self-cleaning surfaces, photoactive decomposition against organic pollutants, and most importantly resistance to moisture and moist-air penetration characteristics. The polyurethane foam surfaces are hydrophobic and naturally resist the moisture. However, in many practical or service conditions, over a period of time, especially when they are exposed to rainy and high humidity atmospheres, as well as indoor conditions having wet atmosphere and improper ventilations, every chance is there for the fungus to grow.

Nanometric oxides like TiO_2, SiO_2, and ZnO and their hybrids are found successful to produce hydrophobic, eco-friendly functional coatings.[1–3] Hydrophobic nature is particularly important in textiles because cottons and synthetic textiles build up static charges due to moisture. Cotton textile fabrics are porous in nature and readily absorb moisture in humid conditions. The moist-air favors bacteria and fungus growth which in turn causes severe breath- and skin-related health hazards. Organization like Cotton Research Institute in India has been developing health-care functional coatings on textiles using TiO_2, ZnO, and SiO_2 hybrids. In addition to the antimicrobial, antifungal, and antistatic characteristics, they also offer UV-blocking property.[4–6] UV shielding sunscreen surface coatings on textiles help to protect human skin from sun burn and skin-cancer. Nano TiO_2/Ag, ZnO/SiO_2/polyester hybrids, and ZnO-starch composites are being tested as UV shielding textile coatings.

ZnO/TiO_2 nanocomposites are better candidate for UV active self-cleaning surface coatings. Concerning the photoactivity, TiO_2 is more effective only when the TiO_2 precursor coatings are heat treated at $\sim 400^{\circ}C$.[7,8] It complicates more to adopt the UV-active TiO_2 coatings for soft surfaces like textiles. Functional nano-ZnO has advantages over TiO_2 because ZnO can block

Correspondence to: S. Ananthakumar (ananthakumar70@gmail.com).

UV in the entire ranges (UV-A, UV-B, and UV-C). It also exhibits antibacterial property in neutral pH even with low quantity of ZnO. Moreover unlike TiO_2 nanoparticles, the ZnO nanocrystals can be easily grown by varieties of chemical techniques at mild synthesis conditions using cheap precursors.

ZnO nanoparticles in different morphologies ranging from rods, tubes, discs, spheres to wires, and arrays have been easily synthesized by surfactant-assisted precipitation followed by low temperature thermolysis ($\sim$ 80°C) and hydrothermal processes ($\sim$ 120°C).[9–13] Surfactant-assisted synthesis has claimed monodisperse nano-ZnO with particles diameter $<$ 10 nm.[14] Encapsulation of ZnO precursor in biopolymer media followed by mechanical activation is an efficient technique to generate *in situ* nucleation and growth of nanocrystals. This has been attempted in this work for obtaining size and shape controlled nano-ZnO through biopolymer-mediated sonochemical technique.

The high energy chemistry explains the mechanism involved in the sonochemical technique. Accordingly, the formation and growth of gas bubbles takes place first, which occurs through the diffusion of solute vapor to the volume of the bubble. When the size of the bubble reaches a maximum value it collapses. The collapse of bubbles in a multibubble cavitation field produces hot spots with effective temperatures of $\sim$ 5000 K, pressures of $\sim$ 1000 atmospheres, and heating and cooling rates above 10^{10} K/s. These extreme conditions are favorable for the nucleation and growth of the nanoparticles.[15]

Polymer foams are usually hydrophobic and physical binding of inorganic nanoparticles with foams is ensured by adhesive nature of the biopolymers. The incorporation of biopolymer is only $<$2 wt % that does not affect the inherent foam-softness.

We selected starch, gelatin, chitosan, and agar biopolymers media to synthesize nano-ZnO directly by sonochemical treatment. The effect of biopolymer templates in the *in situ* ZnO particle growth, evolution of particle morphology, and rheology has been studied. Furniture-grade polyurethane foam was provided with these biopolymer-ZnO nanocomposites coatings and the UV photoactivity and antifungal properties were tested. The study shows that biopolymer-mediated sonochemical is a facile technique for obtaining ZnO colloids that can be directly employed for surface engineering of soft surfaces. It is also a viable process for small- and medium-scale industries to develop attractive "nanoproducts."

EXPERIMENTAL

Zinc nitrate hexahydrate (Merck, India, 99%), starch and gelatin (s.d. fine CHEM LTd, India), chitosan and agar (Rankem, India) were used in as received conditions. Except chitosan, other biopolymers (0.5 g) were dissolved in 100 mL water. Stable starch and agar solutions were prepared by heating the solution at 80°C followed by cooling. A stable, transparent gelatin colloid was prepared by warming the solution at $\sim$ 60°C. In the case of chitosan, a clear solution was obtained by dissolving 0.125 g of chitosan in 100 mL of 2% acetic acid–water solution. Zinc nitrate hexahydrate precursor equivalent to 0.1*M* was dissolved in 100 mL biopolymer solution by mechanical stirring. After it completely dissolved, 0.2*M* NaOH solution was added dropwise under constant stirring to make pH $\sim$ 9. The whole mixture was subjected to sonication for 1 h using bath-type sonicator (Oscar ultrasonic cleaner 37 kHz, 80 W) at room temperature. The initial temperature of the reactants solution was measured as 27°C which was increased to 59°C after an hour sonication. From this solution, white precipitate was separated centrifugally and washed with distilled water to remove the soluble impurities. The final product was then dried at 70°C for 10 h and then subjected to phase purity, thermal stability, structural bonding characteristics, particle size distributions, morphology, and rheology characterizations. For the coating application, the sonicated ZnO-biopolymer colloidal suspension was directly utilized.

Characterization techniques

Thermal decomposition was analyzed by a Shimadzu Thermal Analyzer, Japan (Model 50H) in air atmosphere at a heating rate of 10 °C min^{-1}. The phase analysis was performed by powder X-ray diffraction (XRD) technique (PW 1710, Philips diffractometer, the Netherlands) using Ni-filtered CuKα radiation (wavelength, λ = 1.5406 Å). The crystallite size was calculated using the Debye–Scherrer formula, $D = 0.9\lambda/\beta \cos\theta$, where D is the crystallite size, λ the wavelength of the X-ray used, θ the Bragg angle, and β line broadening. The value of β is usually measured from the peak width at half the peak height. Fourier transform infrared (FTIR) spectra were recorded using a Nicolet Magna-IR 560 spectrophotometer (KBr pellets as standard) in the range of 400–4000 cm^{-1}. Viscosity measurements were taken at shear rates 100–1000 s^{-1} using Rheolab MCI viscorheometer (Physica, Anton Paar, Germany). The particle size distribution analysis was performed using Malvern Zeta sizer. The particle morphology was observed using scanning electron microscope (SEM, Hitachi, 2240 Japan). A transmission electron microscope (FEI, TECNAI 30S-Twin, the Netherlands) with an accelerating voltage of 300 keV was used to obtain the TEM micrographs. Samples were mounted on carbon coated Cu-TEM grids for this purpose. The mechanical stability of the biopolymer-ZnO coatings was ascertained using tensile testing

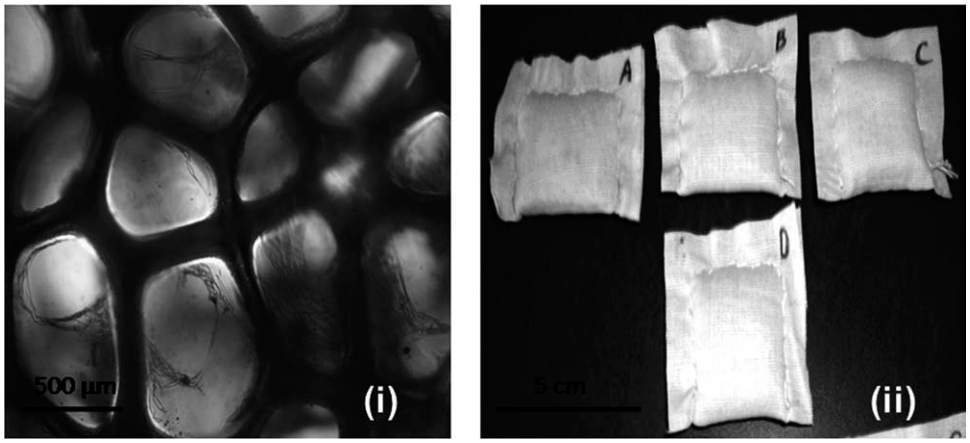

Figure 1 Optical microscopic image of polyurethane foam (i) and the sample pillows, (ii) made with the foam for the fungi growth testing.

conducted over the sample pieces cut from the coated cotton fabrics. Rectangular sample with dimensions of 10 cm length and ~ 2.5 cm width was cut from the coated cotton fabrics and the tensile force was applied at a ramp rate of 2 mm s^{-1}. The rupture time was measured with respect the force (N) versus extension (mm).

Fabrication of coatings

In this work, commercially available polyurethane foam which is regularly used for making comfort furniture was selected. The open cell volume per square inch is ~ 500 cc. Foam cubes having dimensions 5 × 5 cm^2 were cut washed in soap water thoroughly and dried. Similarly, cotton fabric was also washed with dilute soap solution followed by sterilization using spirit before any use. Mini foam-pillows were stitched with a piece of clean cotton cloth and foam. The optical microscopic image as well as the physical appearance of the sample pillows prepared for the fungi growth testing is given in the Figure 1 (i,ii). The coating solution was prepared with 0.2 wt % biopolymer nano-ZnO with 0.2% acrylic binder. The solid to liquid ratio was 1 : 20. The foam pillow cubes were dipped in the coating mixture. The dipping was repeated for at least eight times in order to ensure 100% wet pick-up of the samples. The coated pillow cubes were allowed to dripped-off naturally for removing the excess liquids as well as solid phases. The samples were then dried at 70°C for 24 h.

UV photoactivity of ZnO-biopolymer nanocomposites

The photoactivity of biopolymer-ZnO nanocomposites coated fabric was tested using the Rayonet Photoreactor (the Netherlands) containing 15 W tubes (Philips G15 T8) as the UV-source, which emitted the UV radiation with the wavelength within the range of 200–400 nm (corresponding to the photon energy range of 3.07–6.14 eV) by the well known methylene blue dye decolorization experiment. A known amount of dye was dropped on the cloth surface and then subjected to UV for various time intervals. The decolorization was qualitatively monitored by the reduction in the UV absorption peak height at wave length 320 nm.

Fungal growth test

Fungal growth on the ZnO-biopolymer nanocomposites coated cotton, foam, and the blank controls were investigated using a standard antifungal test procedure.[16] In a typical test, the samples were first sterilized and then treated with ZnO-biopolymer nanocomposites. One set of blank (control) samples were also made. A sterile Petri dish was used for all the antifungal tests. The fungus used for testing was *Aspergillus niger* NCIM 563, commonly found in the environment. The sterilized samples were applied a thin layer of autoclaved potato dextrose agar medium. Then the control and the test sample were sprayed with an equal amount of (500 µL) a fungal spore suspension which was diluted to the range of 2 × 10^5 CFU/mL. The Petri dishes were placed in incubator set at 28°C for monitoring the growth of the fungus. The fungi formation was examined using an optical microscope (Leica—DMRX).

RESULTS AND DISCUSSION

Nanoparticles have high surface area and surface energy where as biopolymers have polymeric forces for excellent adhesion on the substrates. Hence inorganic-biopolymer nanocomposites have more advantages than the single-phase, inorganic nanocolloids for solution coatings and surface engineering. Moreover, the biopolymers control the nucleation and

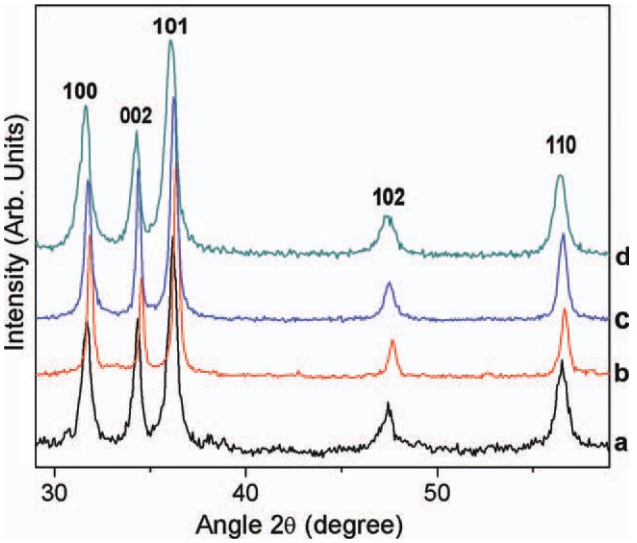

Figure 2 Powder X-ray analysis of nano-ZnO synthesized by biopolymer-mediated sonochemical technique: (a) starch, (b) gelatin, (c) chitosan, and (d) agar media. [Color figure can be viewed in the online issue, which is available at wileyonlinelibrary.com.]

favor directionally oriented growth of nanoparticles. The powder X-ray analysis of ZnO synthesized via sonochemical technique in various biopolymer media is presented in Figure 2. The XRD peaks confirm that sonochemical technique produced well crystalline, hexagonal, wurtzite ZnO directly within 1 h without any additional heating. It is to mention that the samples were only subjected to 10 h drying at 70°C. All the peaks show characteristic ZnO and can be indexed to (100), (002), (101), (102), and (110) crystal planes at corresponding 2θ values of 31.7, 34.4, 36.2, 47.5, and 56.6, respectively. The XRD results are in good agreement with the standard ZnO JCPDS file 89-0510.

The sequential reactions involved in the formation of ZnO are well established and the chemical reactions that usually occur are given below.[17,18]

$$Zn(NO_3)_2.6H_2O + 2NaOH \rightarrow Zn(OH)_2 + 2Na(NO_3) + 2\,H_2O \quad (1)$$

$$Zn(OH)_2 + 2\,H_2O \rightarrow [Zn(OH)_4]^{2-} + 2H^+ \quad (2)$$

$$[Zn(OH)_4]^{2-} \rightarrow ZnO + H_2O + 2OH^- \quad (3)$$

$$Zn^{2+} + 2 \cdot O_2^- \rightarrow ZnO + 3/2\,O_2 \quad (4)$$

As expected, the base addition controlled the pH and hydrolyzed the precursor to form $Zn(OH)_2$. However, sonication transforms $Zn(OH)_2$ precipitate to fully crystalline ZnO. Unlike other solution-growth techniques like precipitation, sol–gel, and polymer complexation, the transformation mechanism is quite different in sonication technique. In conventional techniques, the hydroxide is usually converted to crystalline ZnO by heating at 500°C. In sonication, the hydroxide to oxide transformation is achieved by the microthermal heating generated out of ultrasonication energy. Also, it has been reported that sonolysis of water under air atmosphere generates the species such as ·H, ·OH, $\cdot O_2^-$ and $\cdot HO_2$.[19,20] The driving forces for the nucleation and growth of crystalline ZnO are the hot-spot generation as well as molecular agitation in ultrasonic cavitations. The influence of biopolymers has been clear from the ZnO crystallites sizes. The ZnO crystallite sizes were determined as 15, 26, 19, and 12 nm for the starch-, gelatin-, chitosan-, and agar-mediated samples, respectively. The biopolymer-assisted sonication resulted in controlled nucleation and growth possibly due to their thermophysical properties, mainly the specific heat (C_{sp}), solubility, and stability during sonication. Since microthermal gradient is the primary cause for the nuclei to form, the C_{sp} of the water–biopolymer system has high relevance in deciding the growth of ZnO particles. Studies have earlier been attempted to determine the C_{sp} values of biopolymer–water mixtures to understand the gelling behavior. The C_{sp} values proportionally increase with temperatures even at low concentrations. It is known that water has high C_{sp} value that increase with temperatures. In this work, we monitored the temperature during sonication synthesis and found that the system temperature increased from room temperature to (56 ± 3)°C. At nearly 60°C, the C_{sp} value of water is 4.187 kJ/kg K at 100 kPa. Sonication generates water bubble reactors with extreme pressures where the C_{sp} also reach very high. When the bubbles collapse an exothermic thermal gradients are produced that rapidly accelerate the reaction kinetics for the nuclei to grow. Among these biopolymer templates, the C_{sp} value of agar-water system is close to that of water [C_{sp} agar = 4.12 kJ/kg K at <80°C]. Interestingly this particular system yielded comparatively least ZnO crystallites.

Water-soluble polymers are known stabilizers for obtaining size- and shape-controlled colloidal nanoparticles. However the extent of adhesive/cohesive forces exerted by these macromolecular biopolymer templates resulted in differential rate of agglomeration depending upon their polymer chain-length. This is ultimately reflecting in the bulk ZnO particle size distributions in aqueous medium. The particle size distribution analysis of ZnO-biopolymer nanocomposites are given in Figure 3. The size distribution curves strongly confirm the clustering nature of ZnO particles in all the cases. The cluster size varies between 200 and 600 nm. A very wide size classification is seen in gelatin–water biopolymers. Among the other biopolymer templates used in this work, gelatin has complex supramolecular structure

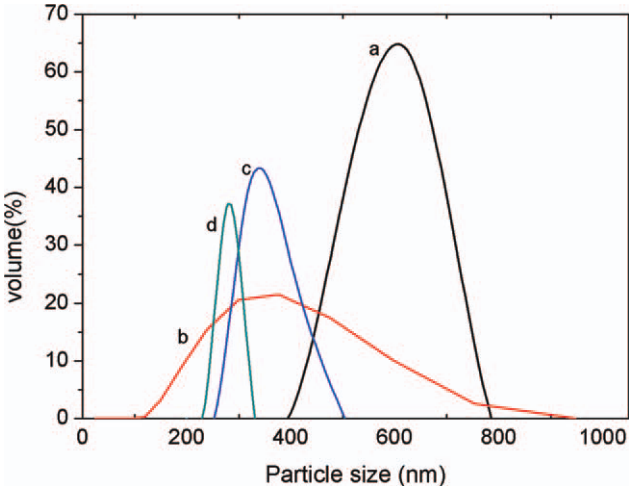

Figure 3 Particle size distribution analyses of ZnO-biopolymer nanocomposite suspensions: (a) starch, (b) gelatin, (c) chitosan, and (d) agar media. [Color figure can be viewed in the online issue, which is available at wileyonlinelibrary.com.]

(collagen-like gel nature) that destabilize with respect to time at elevated sonication temperatures. This resulted in differential rate of nucleation that finally showed wide size particles. In this case the samples have size classifications from 100 nm to nearly a micron.

Even though the biopolymer-mediated sonochemical synthesis produced particles well above the definition of "nano," the starch, chitosan, gelatin, and agar polymers give excellent stability to the ZnO suspensions. These macromolecular biopolymers stabilize ZnO particles through "steric" mechanism. The extent of ZnO–biopolymer interactions can be understood by the viscosity data presented in Figure 4 (i,ii).

In all the cases, the flow curves show Newtonian-type behavior. The rheo-curves observed at different shear rates show linear stress-dependence and the resistance offered for the flow is minimum in starch biopolymers and maximum for the agar polymer as expected [Fig. 4(i)]. ZnO-Agar suspensions developed high stress even at high shear rates. For a functional coatings, an easy spreading as well as firm adhesion is necessary and the flow curves indicate that the increase in viscosity and stress follows the order as starch < chitosan < gelatin < agar. The flow curves in Figure 4(ii) show gradual decrease in viscosity values at increased shear rates. The flow curves have similar trends, i.e., low viscosity for starch and high viscosity for agar biopolymers. The viscosity and stress development lies in the mechanochemical stability of the structure of the biopolymers as well as the particle morphology of ZnO. In all these cases, the ZnO solid fraction (2 wt %), sonication time, temperature as well as the volume (25 mL of 0.2 wt % solution) was maintained at identical conditions. Therefore, the flow-behavior of the biopolymer-ZnO suspension has to be correlated with only the influence of *in situ* sonication energy on the macromolecular structure, tendency for the structure collapse or de-bonding, and de-clustering of ZnO agglomerations. Starches depending upon the source vary widely in the structure and compositions, but mostly they consist of two major molecular components, amylose (20–30%) and amylopectin (70–80%), both of which are polymers of α-D-glucose units.[21] Starch suspensions in water acquire hydrated or hydrogen bonding and its regular structure enables this polymer to form H-bridges over large parts of the molecule together with other amylose molecules. The mutual formation of H-bridges in the full length of the molecule is possible only at sufficiently high concentrations. However, in this work only a weak H-bridge network is possible that readily collapse during sonication and de-agglomeration takes

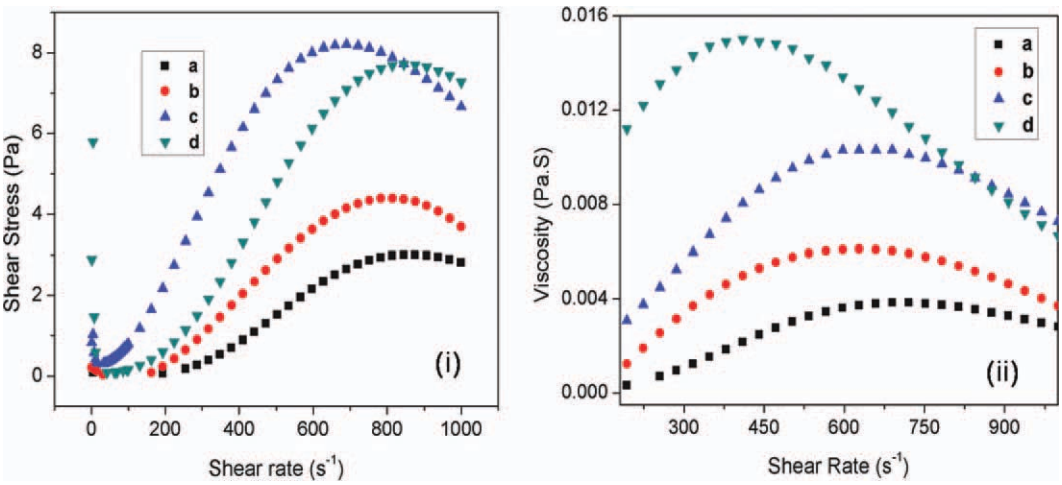

Figure 4 Flow behavior of biopolymer-ZnO aqueous solutions: (a) starch (b) chitosan (c) gelatin, and (d) agar. [Color figure can be viewed in the online issue, which is available at wileyonlinelibrary.com.]

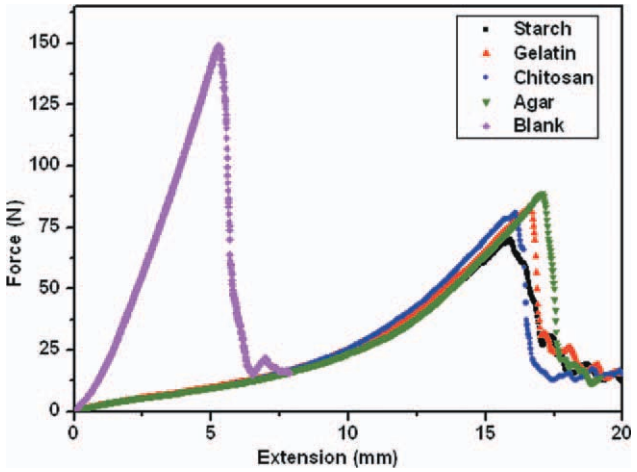

Figure 5 The mechanical degradation curves obtained from the tensile testing conducted over rectangular shape cotton sample pieces. [Color figure can be viewed in the online issue, which is available at wileyonlinelibrary.com.]

place that result in low viscosity and stress. Gelatin, a fibrous protein, is an amphiphilic electrolyte with active terminal amino groups and polypeptide linkages, which mostly serves as a stabilizer. Gelatin is a rigid-chain, high molecular weight compound and its macromolecules exhibit typical elastic texture-like linear-chain synthetic polymers in aqueous medium. Structurally, gelatin molecules contain repeating sequences of glycine-X-Y triplets, where X and Y are frequently proline and hydroxyproline amino acids.[22] These sequences are responsible to form gels in water at appropriate temperature and concentrations. Due to rigid long-chain nature, the changes in molecular shape and charge distribution of the gelatin molecules are difficult even under sonication. This is a reason for comparatively high viscosity of gelatin-ZnO suspensions. The structure of chitosan and its interaction in aqueous solution is studied earlier and reported.[23] Chitosan is composed by a string of blocks of almost fully deacetylated polysaccharide stretched by electrostatic repulsion, intercalated with micelle-like agglomerates formed by almost fully acetylated polysaccharide. These agglomerates include $-NH_3^+$ groups which produce electrostatic swelling of the agglomerates. The rheobehavior of chitosan solution depends on the deacetylation degree due to mechanical agitation and temperature of the solution. Agar is a very heterogeneous molecule. The agar usually exists in the form of neutral agarose, which is an alternating polymer of D-galactose and 3,6-anhydro-L-galactose. A very high viscosity in agar solution is due to its increased level of anhydro bridging in the molecule which is responsible for the inherent gelling fraction of the agar. The inherent viscous nature of the biopolymer is in fact important because it decides the spreading, extent of adhesion as well as the thickness of the coatings. This is confirmed from the mechanical stability test conducted on the cotton cloth coated with these biopolymers. The mechanical degradation curves obtained from the tensile testing conducted over rectangular shape cotton sample piece are shown in Figure 5.

The uncoated bare cotton cloth ruptured catastrophically where as a much delayed rupture occurred in the biopolymer coated fabrics. The time-delay in rupturing was comparatively high for the agar biopolymer which is quite viscous in nature under identical conditions. Among the bio-polymers employed here, starch gives much early failure when the tensile force is applied. A similar mechanical stability also over the porous polymer foams is expected.

The structure–bonding and interactions of the biopolymer macromolecules have been further elucidated in FTIR analysis which is presented in Figure 6. The starch, gelatin, chitosan, and agar biopolymers are extremely important to food and agro-products and numerous studies have reported the FTIR finger prints of the stretching and bending frequencies of these biopolymers. The results seen in the FTIR frequencies have been well matching with the reported data.[24] The FTIR spectra corresponding to ZnO-starch composite (a) (Fig. 6) revealed a high intensity band at 2930 cm^{-1} representing the characteristic C—H stretching associated with hydrogen atoms and the band at 1150 cm^{-1} was attributed to C—O bond stretching of C—O—H group. The peak at 1080 cm^{-1} was assigned to C—O bond stretching of C—O—C group in the anhydro glucose ring of starch. The ZnO-gelatin composite samples (b) (Fig. 6) have peak

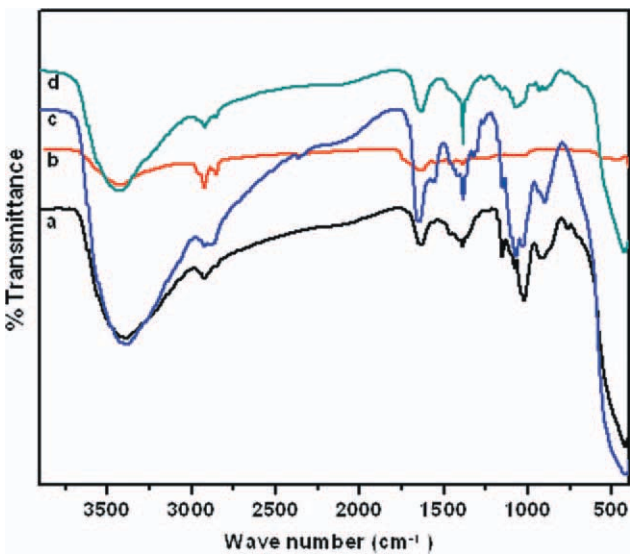

Figure 6 FTIR spectra of ZnO-biopolymer composites dried at 80°C/24 h. (a) ZnO-starch, (b) ZnO-gelatin, (c) ZnO-chitosan, and (d) ZnO-agar. [Color figure can be viewed in the online issue, which is available at wileyonlinelibrary.com.]

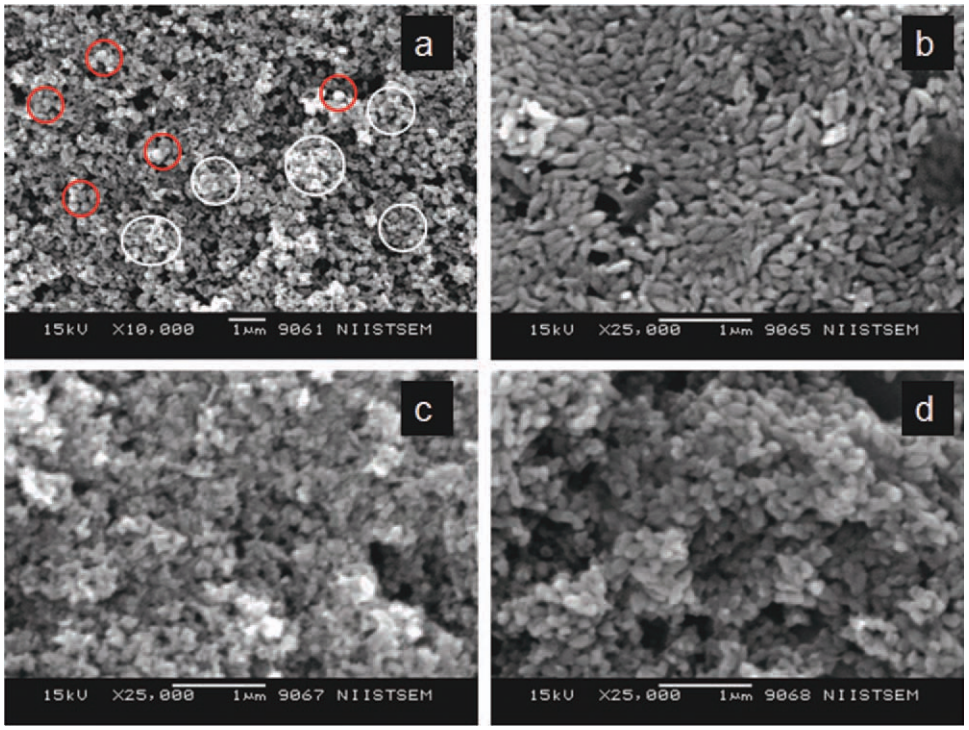

Figure 7 Morphologies of ZnO-biopolymer nanocomposites prepared with (a) starch, (b) gelatin, (C) chitosan, and (d) agar templates. [Color figure can be viewed in the online issue, which is available at wileyonlinelibrary.com.]

at 3430 cm^{-1} due to —NH stretching of secondary amide group in gelatin. The peak at 1635 cm^{-1} corresponds to C=O stretching, characteristic for the coil structure of gelatin. The peak at 1550 cm^{-1} can be attributed to —NH bending. The samples also show C—H stretching peaks at 2922 cm^{-1} and 2850 cm^{-1}, respectively. The peak at 670 cm^{-1} can be ascribed to the —NH out-of plane wagging.[25] Similarly, the FTIR spectra of ZnO-chitosan composite (c) (Fig. 6) shows a broad band at $\sim$ 3440 cm^{-1} corresponding to the stretching vibration of N—H. The peaks at 2924 cm^{-1} and 2846 cm^{-1} are typical of C—H stretch vibration, while peaks at $\sim$ 1639 cm^{-1}, 1540 cm^{-1}, and 1317 cm^{-1} are characteristic of amide I, II, and III, respectively. The sharp peaks at 1420 cm^{-1} and 1383 cm^{-1} are assigned to the CH_3 symmetrical deformation mode and 1153 cm^{-1} and 1088 cm^{-1} are indicative of C—O stretching vibrations (C—O—C). The small peak at $\sim$ 900 cm^{-1} corresponds to the wagging of saccharide structure of chitosan.[26] The most prominent band in the FTIR spectra of agar biopolymer centered at $\sim$ 1079 cm^{-1} has contributions from several vibrational modes, namely to the C—O and C—C stretching and to the C—C—O and C—O—H deformations. The presence of a strong band at 930 cm^{-1} is the indicative of the occurrence of 3,6-anhydro-D-galactose.[27] In all the biopolymer-ZnO samples, FTIR band peaks at 420, 423, and 464 cm^{-1} are indicating the characteristics of ZnO. The FTIR analysis confirm that in the nano-ZnO particles there was strong binding, but no obvious formation of covalent bonds between soluble biopolymers and ZnO.

The nature of the biopolymer structures as well as their complexation with the Zn-metal ions followed by the degree of nucleation and growth produced definite variations in the final morphology of ZnO particles. The morphologies of ZnO particles by the effect of biopolymer templates as observed by SEM are shown in Figure 7. All the samples show agglomerated ZnO nanoparticulate micro/nanoclusters because of their polymeric forces. The starch-mediated samples contain isolated spherical-shaped particles as well as aggregates composed of several ZnO nanoparticles. The spherical particles (marked in small red color circles) are actually starch which has size about 200 nm. The clusters or aggregates have size close to one micron (marked in large white color circles). These clusters consist of many nano-size ZnO crystallites. These nanocrystals have average size $<$ 50 nm. The gelatin-templated ZnO particles attained rice-like nanograins with average dimension of 100 nm. They also horizontally orientated to the substrates. The chitosan-derived ZnO clusters show nanospheres. However, these nanoclusters revealed porous agglomerates of larger sizes. The agar-derived ZnO particles have egg-shaped nanocrystals close to size 50 nm. The nano morphologies were further clarified by the transmission electron microscopy (TEM) analysis and the results are shown in Figure 8.

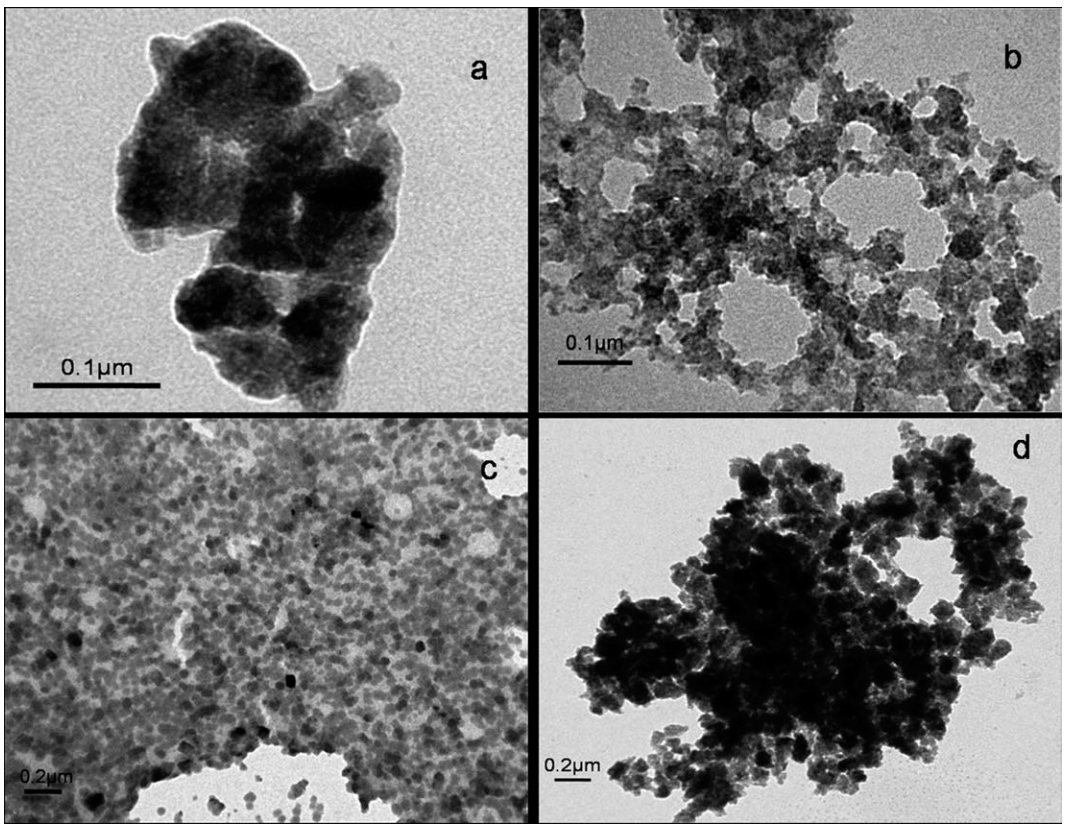

Figure 8 TEM images of ZnO-biopolymer nanostructures synthesized by sonochemical method with (a) starch, (b) gelatin, (C) chitosan, and (d) agar.

TEM images of the biopolymer-mediated sonochemically processed ZnO particles have 80, 41, 38, and 60 nm for the starch, gelatin, chitosan, and agar, respectively. These nanoparticles are stable under the electron beams used for TEM measurements, indicating a strong binding between the ZnO and biopolymers. These values are on the higher side compared to the crystallite sizes observed by XRD indicating the extent of agglomeration by the biopolymers. The morphologies as well as the aggregations of ZnO nanoparticles could be attributed by the complexation nature of biopolymers with ZnO divalent metal ions, their high number of coordinating functional groups (hydroxyl and glucoside groups) encapsulation and immobilization capacity, ability of amylase to form coil structure, the presence of the large number of functional side groups (mainly in gelatin), and finally the chemical crosslinking.[21,28]

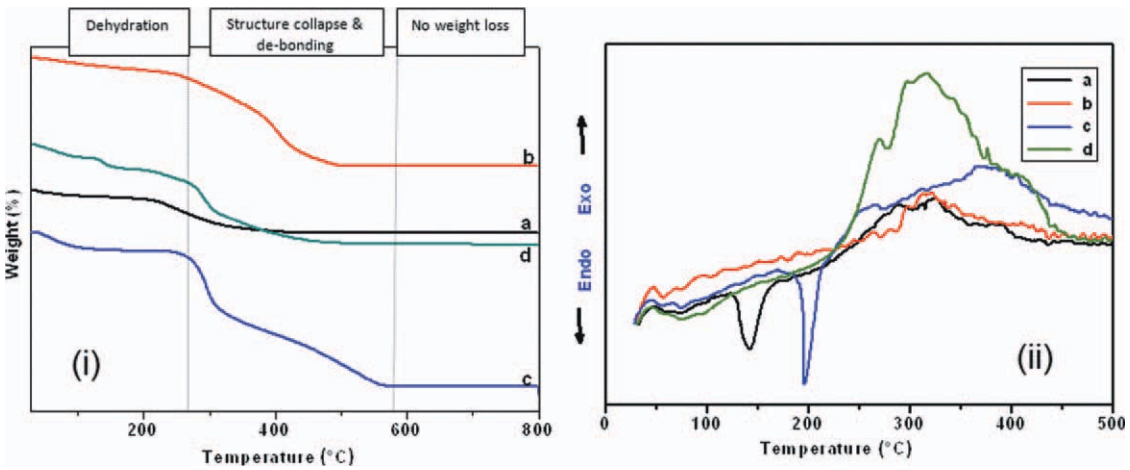

Figure 9 TG/DTA Thermograms of ZnO-biopolymer nanocomposites: (a) starch, (b) gelatin, (c) chitosan, and (d) agar. [Color figure can be viewed in the online issue, which is available at wileyonlinelibrary.com.]

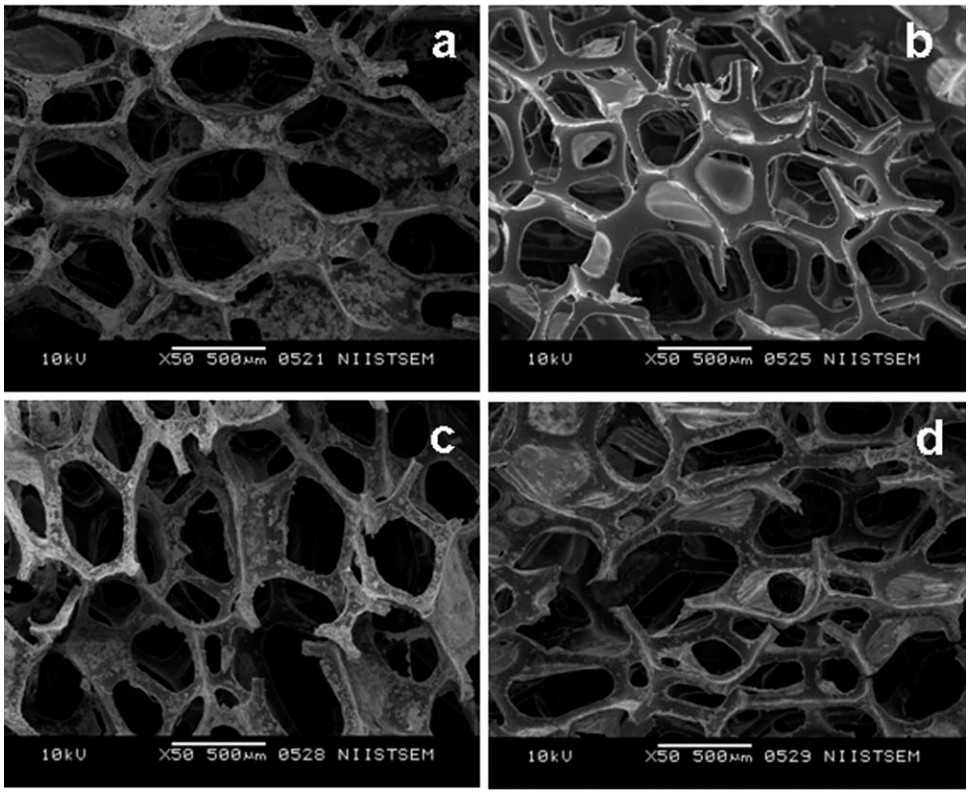

Figure 10 SEM micrographs of polyurethane foams coated with ZnO-functional biopolymers: (a) starch, (b) gelatin, (c) chitosan, and (d) agar.

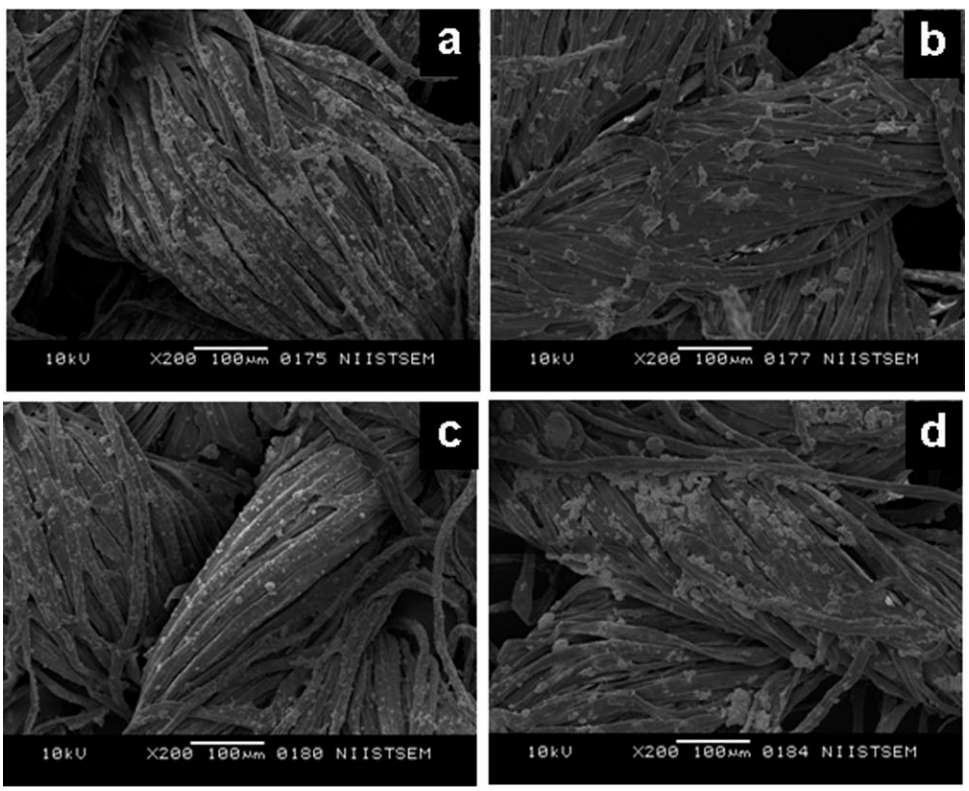

Figure 11 SEM micrographs of the cotton fabrics applied with ZnO-biopolymer coatings.

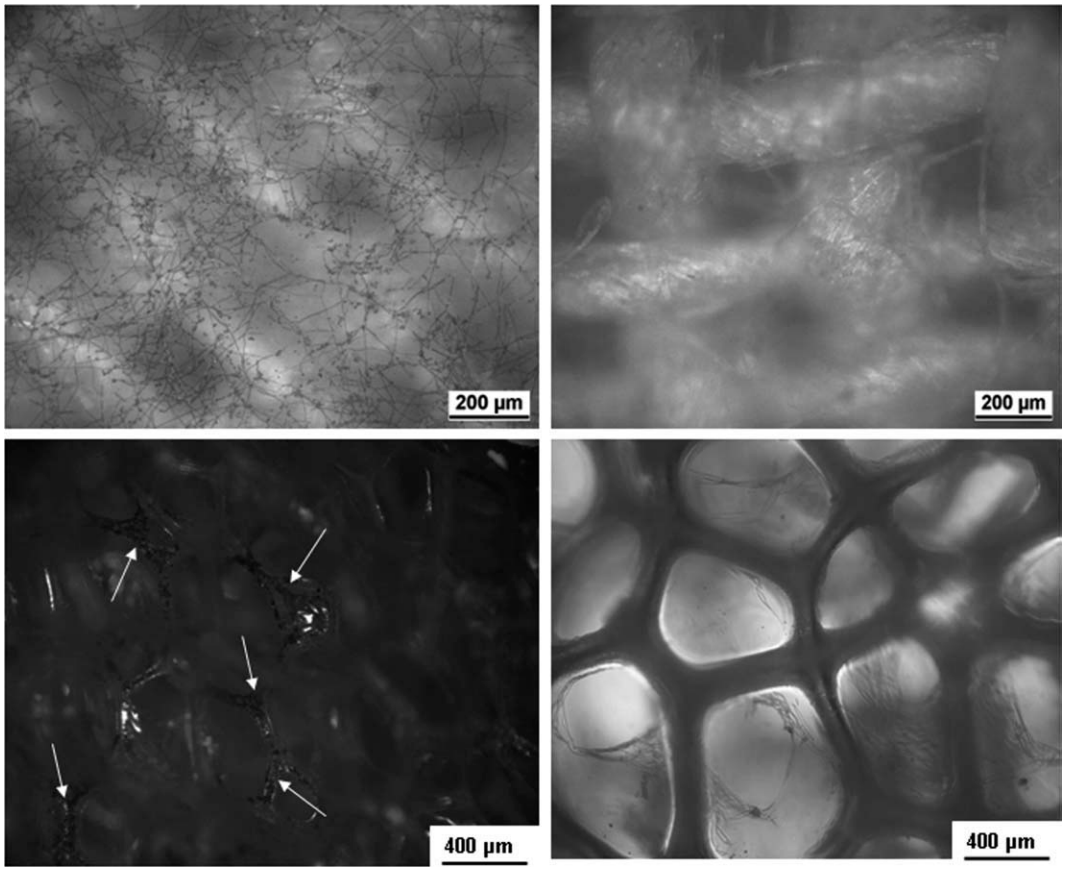

Figure 12 Optical microscopic images of representative agar-ZnO nanocomposites coatings on cotton and polyurethane foam after fungi test. Left: Coated only with agar Right: coated with agar-ZnO nanocomposite.

Chitosan has a remarkable ability to form specific complexes with a number of ions including transition and post-transition metal ions.[29] It is known that the free amino groups of chitosan are responsible for its complexing behavior with ions. The aggregation of the ZnO nanoparticle in agar medium is decided by the formation of macro-reticulated gel network by the agar molecules.

The polymer decomposition and the weight fraction of nano-ZnO contents have been analyzed in the ZnO-biopolymer composites through thermogravimetric analysis (TG and DTA) under nitrogen atmosphere and the results are shown in Figure 9(i,ii). On the TGA curves, a weight loss below 200°C was associated with the loss of adsorbed and bound water (dehydration). At temperatures 200–500°C, the rate of decomposition and weight loss is maximum that mainly corresponds to the degradation of polymer matrices. Under the nitrogen flow, a non-oxidative degradation occurs. The percentage yield of ZnO was calculated from the weight loss of the biopolymer at these temperatures. It was determined as 79.24, 67.83, 83.17, and 60.05 wt %, respectively, for the starch, gelatin, chitosan, and agar polymers. The maximum yield was observed for ZnO-chitosan composite. ZnO-agar composite showed comparatively low conversion of ZnO. The DTA analyses confirm that the polymer decompositions occur at these temperature intervals.

The microstructures of the ZnO-biopolymer coatings developed on the polyurethane foams and cotton fabrics are shown in Figures 10 and 11, respectively. The starch and chitosan biopolymers have shown homogeneous adhesion of nano-ZnO that completely spread through the foam-walls. These images further reveal that the ZnO nanoparticles are firmly held on the coatings with adequate thickness. The polymers were also found to maintain the softness at these stages. The gelatin and agar polymers show continuous film-like growth rather than the preferred particle adhesions. The microstructures of cotton fabrics show that the nano-ZnO also gets attached uniformly with the surfaces of the cotton fabrics. In starch and agar suspensions, the particle adhesion is excess but the chitosan and agar polymers show thin layer of nano-ZnO adhesions.

The results on the fungi growth characteristics under the given testing conditions over the surfaces of the polyurethane foam as well as on the cotton fabrics are shown in Figure 12. We display here the representative images from agar-ZnO biopolymer nanocomposites for explaining the fungus growth

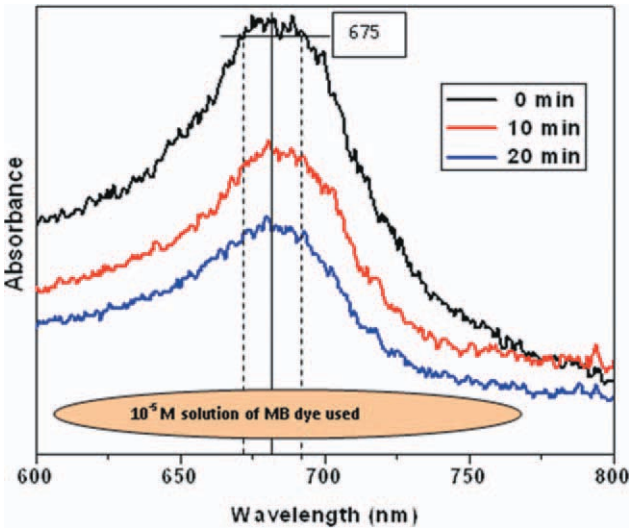

Figure 13 UV photoactivity of the ZnO-starch nanocomposite coatings on cotton substrates. [Color figure can be viewed in the online issue, which is available at wileyonlinelibrary.com.]

resistance. Compared to other biopolymers, agar is the favorable medium for the fungi to grow. The surface topologies of the uncontrolled blanks in which only agar solution was applied without any ZnO revealed fungus growth on both the cotton as well as polymer foam surfaces at given experimental conditions. Black fungus spores have been seen in the optical microscopic images. The samples applied with ZnO containing agar coatings have no significant growth indicating the efficiency of the ZnO-biopolymer nanocomposites.

The UV photoactivity of the ZnO-biopolymer nanocomposites was tested on the ZnO-coated cotton substrates. In fact, the powder X-ray analysis of the coated cotton substrates confirmed the presence of nanocrystalline ZnO in the coatings. The UV absorbance of the ZnO-biopolymer-coated cotton samples soaked in the methylene blue (MB) dye solution (10^{-5} molar concentration) was tested before and after UV reactions (Fig. 13). The MB dye absorbance peak intensity (675 nm) was reduced with time indicating the MB dye decomposition due to the photochemical activity of the ZnO. UV photoactivity further shows possibilities that the fungus spores can be completely removed or decomposed from the foams and cotton fabrics by periodic cleaning using UV.

CONCLUSIONS

A facile, one-step synthesis of nanocrystalline ZnO was prepared using biopolymer-mediated sonochemical technique at <60°C. The micro-thermal heating generated from the ultrasonic cavities transform the hydrolyzed $Zn(OH)_2$ to crystalline ZnO within 1 h sonication. The biopolymer-mediated sonication resulted in morphologically varied nanocrystalline ZnO. Morphologies such as microspherical nature, rice-like particles, nanospherical clusters, and well-defined egg-shaped ZnO crystals have been observed when starch gelatin, chitosan and agar biopolymers are employed. All biopolymer templates resulted in ZnO clusters of size ~ 600 nm. However the SEM/TEM analysis showed the ZnO particles have sizes <100 nm. A smallest particle size of 41 nm was seen in chitosan-mediated synthesis. Stable ZnO colloid was obtained by the steric stabilization of macromolecular biopolymers. The viscosity measurements revealed non-Newtonian flow behavior. The agar suspension had comparatively high viscosity. However, all suspensions exhibit free-flow for the application of coatings. Thermogravimetry analysis confirmed the ZnO yield in the range 60–80 wt % depending on the nature of the biopolymer. ZnO-biopolymer nanocomposite coatings applied on cotton-covered polyurethane foam showed multifunctional properties like UV photoactivity and strong resistance to fungus growth. The study shows possibility to develop water-free, UV-assisted self-cleaning textiles and foams.

References

1. Fei, B.; Deng, Z. X.; Xin, J. H.; Zhang, Y. H.; Pang, G. Nanotechnology 2006, 17, 1927.
2. Wang, Z. Y.; Han, E. H.; Ke, W. Polym Degrad Stab 2006, 91, 1937.
3. Xu, T.; Xie, C. S. Prog Org Coat 2003, 46, 297.
4. Wang, R. H.; Xin, J. H.; Tao, X. M.; Daoud, W. A. Chem Phys Lett 2004, 398, 250.
5. Vigneshwaran, N.; Kumar, S.; Kathe, A. A.; Varadarajan, P. V.; Prasad, V. Nanotechnology 2006, 17, 5087.
6. Farouk, A.; Textor, T.; Schollmeyer, E.; Tarbuk, A.; Grancacic, A. M. Autex Res J 2009, 9, 114.
7. Xu, Y.; Wang, H.; Wei, Q.; Liu, H.; Deng, B. J Coat Technol Res 2010, 7, 637.
8. Inagaki, M.; Hirose, Y.; Matsunaga, T.; Tsumura, T.; Toyoda, M. Carbon 2003, 41, 2619.
9. Meen, T. H.; Water, W.; Chen, Y. S.; Chen, W. R.; Ji, L. W.; Huang, C. J. IEEE International Conference On Electron Devices and Solid-State Circuits, Tainan, vols. 1 and 2, Proceedings, 2007; p 617.
10. Yu, H. D.; Zhang, Z. P.; Han, M. Y.; Hao, X. T.; Zhu, F. R. J Am Chem Soc 2005, 127, 2378.
11. Anas, S.; Mangalaraja, R. V.; Ananthakumar, S. J Hazard Mater 2010, 175, 889.
12. Khomenkova, L.; Fernandez, P.; Piqueras, J. Cryst Growth Des 2007, 7, 836.
13. Xu, L. F.; Chen, Q. W.; Xu, D. S. J Phys Chem C 2007, 111, 11560.
14. Cao, X.; Wang, N.; Wang, L. Nanotechnology 2010, 21, 065603.
15. Suslick, K. S.; Price, G. J. Annu Rev Mater Sci 1999, 29, 295.
16. Lass-Florl, C.; Cuenca-Estrella, M.; Denning, D. W.; Rodriguez-Tudela, J. L. Med Mycol 2006, 44, S319.
17. Li, W. J.; Shi, E. W.; Zhong, W. Z.; Yin, Z. W. J Cryst Growth 1999, 203, 186.
18. Jung, S.-H.; Oh, E.; Lee, K. H.; Yang, Y.; Park, C. G.; Park, W.; Jeong, S. H. J Cryst Growth Des 2008, 8, 265.

19. Destaillats, H.; Colussi, A. J.; Joseph, J. M.; Hoffmann, M. R. J Phys Chem A 2000, 104, 8930.
20. Destaillats, H.; Lesko, T. M.; Knowlton, M.; Wallace, H.; Hoffmann, M. R. Ind Eng Chem Res 2001, 40, 3855.
21. Mishra, P.; Yadava, R. S.; Pandey, A. C. Dig J Nanomater Bios 2009, 4, 193.
22. Bigi, A.; Panzavolta, S.; Rubini, K. Biomaterials 2004, 25, 5675.
23. Desbrieres, J. Polymer 2004, 45, 3285.
24. Sreeram, K. J.; Ramasamy, I.; Nair, B. U. Transition Met Chem 2008, 33, 127.
25. Payne, K. J.; Veis, A. Biopolymers 1988, 27, 1749.
26. Li, Y.; Wu, K.; Zhitomirsky, I. Colloids Surf A 2010, 356, 63.
27. Pereira, L.; Sousa, A.; Coelho, H.; Amado, A. M.; Ribeiro-Claro, P. J. A. Biomol Eng 2003, 20, 223.
28. Taubert, A.; Wegner, G. J Mater Chem 2002, 12, 805.
29. Ogawa, K.; Oka, K.; Yui, T. Chem Mater 1993, 5, 726.